Strength and Microstructure of Concrete with Iron Ore Tailings as Replacement for River Sand

Ali Umara Shettima[1], *Yusof* Ahmad[2*], *Moh*d Warid Hussin[2], *Nasiru* Zakari Muhammad[2], and *Ogunbode* Eziekel Babatude[2]

[1]Department of Civil Engineering Technology, Federal Polytechnic Damaturu, Yobe State. 620001, Nigeria
[2]Faculty of Civil Engineering, Universiti Teknologi Malaysia, Johor Bahru. 81310, Malaysia

Abstract. River Sand is one of the basic ingredients used in the production of concrete. Consequently, continuous consumption of sand in construction industry contributes significantly to depletion of natural resources. To achieve more sustainable construction materials, this paper reports the use of iron ore tailings (IOT) as replacement for river sand in concrete production. IOT is a waste product generated from the production of iron ore and disposed to land fill without any economic value. Concrete mixtures containing different amount of IOT were designed for grade C30 with water to cement ratio of 0.60. The percentage ratios of the river sand replacements by IOT were 25%, 50%, 75% and 100%. Concrete microstructure test namely, XRD and Field Emission Scanned Electron Microscopic/Energy dispersive X-ray Spectroscopy (FESEM/EDX) were conducted for control and IOT concretes in order to determine the interaction and performance of the concrete containing IOT. Test results indicated that the slump values of 130 mm and 80 to 110 mm were recorded for the control and IOT concretes respectively. The concrete sample of 50% IOT recorded the highest compressive strength of 37.7 MPa at 28 days, and the highest flexural strength of 5.5 MPa compared to 4.7 MPa for reference concrete. The texture of the IOT is rough and angular which was able to improve the strength of the concrete.

1 Introduction

The challenge for the civil engineering community with the concept of sustainable development involves the use of waste materials and by-products at reasonable cost with the lowest possible environmental impact. Rapid increase in consumption of river sand due to the increased in construction activity means that sand mining exploration increased in which the river bed is over exploited [1, 2]. Other environmental issues of Sand mining are depletion of virgin deposits, collapsing of river banks, water table lowering and water pollution [3]. The remedies for these impacts are the use of waste material as alternatives to river sand. Increase in the production of iron ore for economic development worldwide has generated massive amount of iron ore tailing, which are frequently being discarded as wastes. This has led to serious environmental deterioration. A statistical survey has shown

* Corresponding author: a-yusof@utm.my

that 5 to 7 billion tonnes of iron ore tailings were produced yearly worldwide [4]. In spite of such huge amount of iron ore tailings stockpiled as waste, its safe disposal or utilization has remained a major unsolved and challenging task for iron ore industries [5]. The objective of this study is to investigate the performance of concrete with IOT as replacement for river sand in terms of strength and microstructure analysis.

2 Materials and mix proportions

Ordinary Portland cement and natural river sand along with crushed gravel of 10 mm coarse aggregates were locally obtained and used in this study. The IOT was obtained from one iron ore mill in southern State of Malaysia. The chemical composition of natural sand and IOT were determined using X-ray fluorescence (XRF) and the results are shown in Table 1.The physical properties of river sand and IOT were also determined and presented in Table 2. The results of particle size distribution of the river sand and IOT are shown in Fig. 1. FESEM/EDS were determined for river sand and IOT. The results of FESEM/EDS for IOT and river sand are presented in Fig. 2 and 3, respectively. The FESEM/EDS result of IOT consists loose particles, porous and highly rough surface with irregular shape that was well dispersed as shown in Fig. 2, while the river sand had a smoother surface as shown in Fig. 3. The EDS consists of silica (Si), which is prominent element present in both materials with a relative percentage by weight of 57.4% and 61.7% for IOT and river sand, respectively. The other elements that were more prominent in IOT were iron (Fe) and alumina (Al), which was about 8.01% and 5.91%, respectively. The alumina element plays a very important role in the formation of calcium alumina silicate hydrate. The high carbon of IOT has resulted high loss of ignition (LOI) value and consequently high water demand. A Polycarboxylic ether based superplasticizer (Rheobuild 1100) complies with ASTM C494 [6] was used to increase the workability of the mix to avoid increase of water. Five mix proportions were prepared as shown in Table 3. The first mix was control, which is a conventional concrete designated as M0 (i.e. without iron ore tailings), and the other four mixes contained IOT. The river sand was replaced with IOT at replacements levels of 25%, 50%, 75% and 100% and designated as M25, M50, M75 and M100 respectively.

Table 1. Chemical composition of river sand and iron ore tailings.

Chemical composition (%)	SiO	Al_2O_3	Fe_2O_3	CaO	MgO	MnO	K_2O	CUO	ZnO	PbO	SO_3	LOI
River Sand	98	0.4	0.1	0.9	0.2	0.02	1.4	-	-	-	-	0.1
IOT	56	10	8.3	4.3	-	1.7	1.5	0.2	0.1	0.4	-	3.3

Table 2. Physical properties of iron ore tailings and river sand.

Type of test	**Sand**	**IOT**
Bulk Specific gravity	2.6	2.8
Relative density (g/cm^3)	1.64	1.27
Fineness modulus	2.77	1.05
Water absorption (%)	3	7.0

Table 3. Mix proportion of concrete mixes incorporating iron ore tailings.

			Proportion of IOT's				
Description			**M0**	**M25**	**M50**	**M75**	**M100**
OPC (kg/m^3)			380	380	380	380	380
Coarse aggregate (kg/m^3)			1009	1009	1009	1009	1009
Natural sand (kg/m^3)			761	571	380.5	190	-
Iron ore tailings (kg/m^3)			-	190	380.5	571	761
Water (kg/m^3)			230	230	230	230	230
Superplastiizer (%)			0.5	0.5	0.5	0.5	0.5
Slump (mm)			130	110	100	90	80
Compaction factor			0.94	0.94	0.91	0.89	0.85
Concrete fresh density (kg/m^3)	2390	2410	2440	2480	2490		

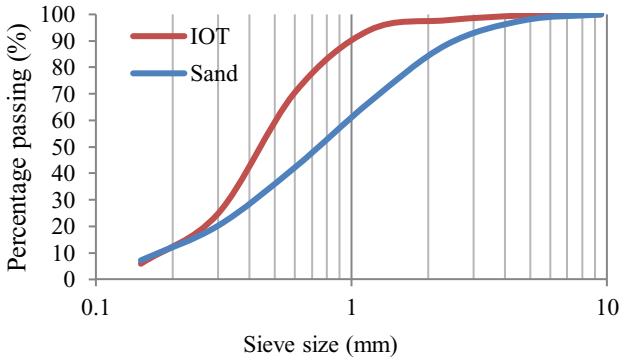

Fig. 1. Grading curve of IOT material and river sand.

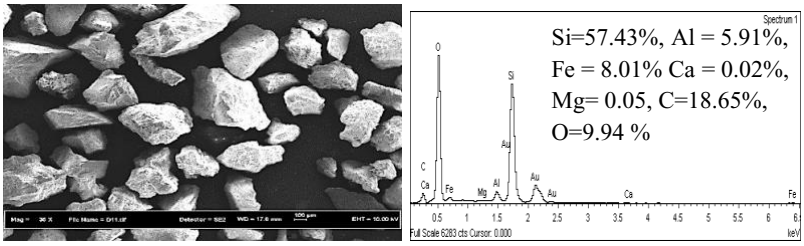

Fig. 2. Energy dispersive X-ray of the spectrum from FESEM of IOT.

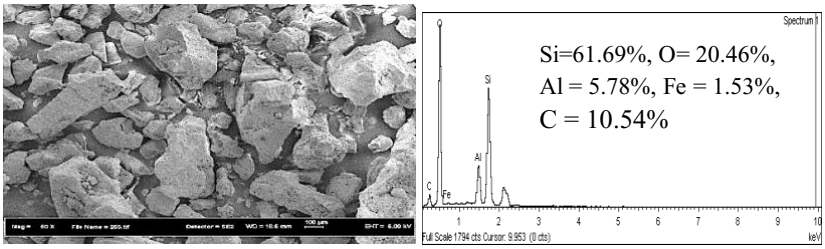

Fig. 3. Energy dispersive X-ray of the spectrum from FESEM of river sand.

2.1 Test method

The slump value, compacting factor value and concrete density of the fresh concrete were determined according to standard specification of BS EN 12350-2 [7], BS 1881-103 [8] and BS EN 12350-6 [9], respectively. The results are presented in Table 3. For each of the concrete mixture, specimens of 100mm cubes for compressive strength and 100x100x500mm prisms of specimens for flexural strength were considered. The Microstructure of the concrete at 28 days with various IOT replacements was analyzed using Field Emission Scanning Electron Microscopy (FESEM) Techniques and X-ray diffraction analysis (XRD). The XRD test was conducted at a source of Cu Kα with 40 KV of X-ray acceleration voltage and 30 mA electric current. The scanning rate was 0.05 °/sec with a scanning interval of 2Θ angle from 5to 65°C.

3 Results and discussions

In this section, properties of concrete in both fresh and hardened form are presented and discussed. Microstructure tests results of XRD and FESEM are also presented and discussed.

3.1 Fresh concrete properties

The results of slump values in Table 3 showed that all the IOT concrete samples reduced the slump value with increase in IOT content due to the high water affinity of the IOT. Although there was decrease in the slump of the IOT concrete samples, but there was improvement in cohesiveness with the addition of superplasticizer. Fresh control concretes (M0) is more cohesive and workable than concrete containing IOT. This might be attributed to the higher specific surface area of IOT, which absorbed more water compared to the river sand. The fineness modulus of 2.07 for IOT; which is less than the minimum value of 2.3 specified for sand by ASTM C33 [10] standard also increased water demand, thus resulting in a decreased in slump workability. The compacting factor test results for all the concrete samples tested, ranges between 0.85-0.94 as shown in Table 3. The British standard BS 1881-103 [8] prescribes for normal weight concrete, compacting factor value range of 0.82 to 0.92.The study of the fresh density of concrete demonstrated in Table 3 shows that fresh density values increase as the IOT content increased in concrete. It can be seen that, although the fresh density was lower in control specimens as compared to those of IOT concrete, all of them are above the minimum limits of 2300 kg/m^3 specified by the BS EN 12350-6 [9]. The higher density values of IOT concrete could be due to the high concentration of iron content in the material, which was heavier than river sand in terms of weight. Another factor could be due to finer particles and angularity which has a better filling effect than the sand, which lead to a higher packing density in the fresh concrete.

3.2 Compressive strength

The compressive strength tests for the control and IOT concrete mixes are shown in Table 4. The results shows that all the IOT concrete samples gave better performance in compressive strength than the control specimen. The incorporation of IOT improves concrete strength up to 50% optimum level and then decreased when the percentage of IOT was more than 50% replacement to sand but still higher than reference concrete (M0). The reasons for this decrease in strength could be attributed to the high water demand for hydration process, which might result to lower compressive strength. The presences of

heavy metals in the IOT such as Zn, Cu, Pb and Cd also retard hydration, and lower the strength development. The percentage increase of compressive strength relative to M0 at 28 days were 6.5%, 13.1%, 9.8% and 7% for M25, M50, M75 and M100, respectively. This observed increase in the compressive strength could be partly attributed to the finer particles of IOT, which filled the pore and optimized the pore structure. It is also attributed to the internal curing effect whereby water from the IOT is gradually released into the concrete to further hydrate the matrix. This may be related to chemistry of IOT as observed in the chemical composition. It is equally suspected that the presence of iron in higher concentrations might have positive effect on strength attainment [11]. It was ranged between 10-50% optimum mixtures replacement of natural sand with IOT [12-15].

Table 4. Compressive strength of concrete specimens.

	Compressive strength of concrete mixes (MPa)		
Type of specimen	**7 days**	**14 days**	**28 days**
M0	23.0	28.8	33.3
M25	25.4	30.7	35.8
M50	26.3	32.6	37.7
M75	24.6	29.6	34.5
M100	23.2	28.9	33.8

3.3 Flexural strength

The flexural strength of concrete specimen with various percentages of IOT is shown in Fig.4. It is observed that the flexural strength gain of the concrete containing IOT was superior to control specimens. It could be seen that, the flexural strength at the age of 28 days, concrete containing 50% IOT for M50 was found to developed higher flexural strength of 13% above that of control concrete M0. In general, concrete containing IOT showed higher rates of flexural strength development throughout the curing period. It is interesting to mention that all the flexural strength of control and IOT concretes were higher than 4 MPa as specified in BS 5328-1 [16].

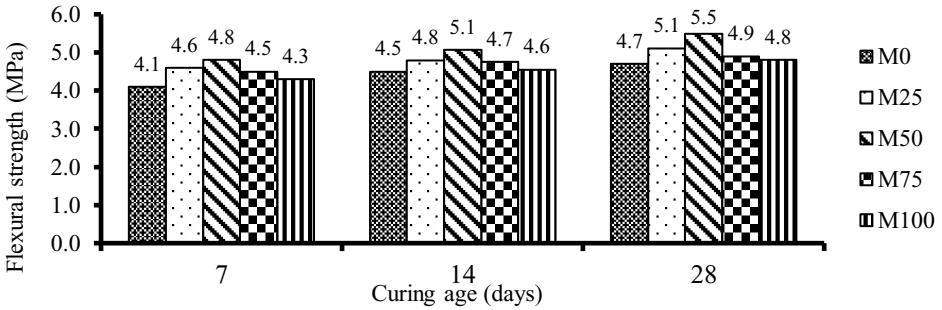

Fig. 4. Flexural strength of respective concrete.

3.3.1 Relationship between flexural strength and compressive strength

The regression line approach was used for the relationship between flexural strength and compressive strength. The coefficient of the linear regression equation with the correlation coefficient for the entire data of the specimens is shown in the Fig.5. Statistical analysis from the equation of the results showed that there is a strong relation between the flexural

and compressive strengths. It can be seen from the figure that the correlation coefficient for flexural strength and compressive was 0.99. The figure also shows that when compressive strength is higher, the flexural strengths were also higher. This relationship is linear form and therefore, it is possible to predict the flexural strength of IOT concrete from its compressive strength using the correlation equations. The result of this study shows that IOT concrete has high potentials to be used in construction requiring flexural resistance.

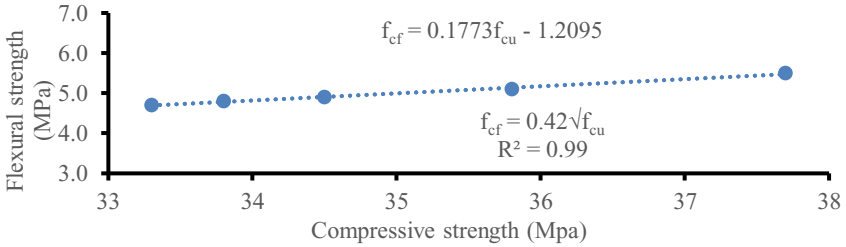

Fig. 5. Relationship between flexural strength and compressive strength.

3.4 X-ray diffraction analysis (XRD)

The XRD microstructural analysis provides useful information on the crystallographic properties of hardened concrete. XRD diffractograms of control specimens and concrete containing IOT at 28 days was presented in Fig. 6. The XRD diffractograms shows the presence of hydrated phases such as quartz (SiO_2), portlandite $Ca(OH)_2$, Dolomite and albite ($NaAlSi_3O_8$) with a peak of calcium silicate hydrate (C-S-H). However, that of IOT concrete mixes contains hematite (Fe_2O_3) in addition to the chemical elements enlisted in the control mixes. The presences of portlandite affected the progress of strength development. The diffraction peak intensity of phase portlandite was more predominant in control concretes as compared to that in IOT concrete samples. The lower portlandite in IOT could be attributed to the reaction between reactive silica in IOT and portlandite which promote the formation of crystallized C–S–H. This reveals that the IOT have the reactivity, as their finer particles are similar to cement or finer than cement.

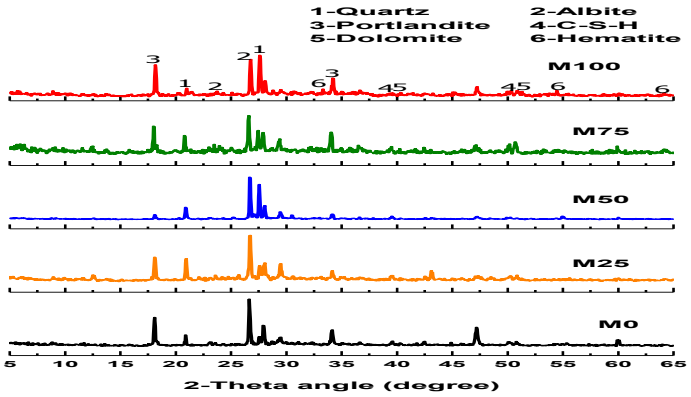

Fig. 6. X-ray diffraction of respective concrete.

3.5 Field Emission Scanning Electron Microscopy

Field-emission scanning electron microscopy (FESEM) provides useful information on the materials and distinguishing morphological features that could be credited to the strength enhancement. Fig. 7 to 11 shows the FESEM morphology of respective concretes.

The morphology of M0 (control specimen) concrete characterised with higher amount of fine needle-like ettringites and porous gaps between the cement and aggregate is shown in Fig. 7. It is also observed that the structures of particles were interconnected and looks like honeycomb with voids. Nonetheless, the microstructure of M25 concrete presented in Figure 8 was relatively less porous with fewer ettringites in the concrete compared with M0. However, there are substantial hexagonal platelets of $Ca(OH)_2$ seen in all the concretes. These $Ca(OH)_2$ crystals were significantly reduced in concrete containing IOT as can be seen from M25 to M100 images. This variation in $Ca(OH)_2$ content can be attributed to the water absorption of IOT materials. It was also noticed that the dark matter in the images stands for IOT. The assumptions regarding the presence of IOT is based on the facts that these medium dark images are seen in almost every sample of IOT except the control specimens. A closer observation indicated that there were no ettringite products in the FESEM of M50, M75 and M100 concretes. Ettringite is generally formed in the early age of hydration and disappeared as the cement hydration continues [17]. This is because after some days depending on the alumina to sulphate ratio of the cement, ettringite become unstable and decomposed to form monosulfoaluminate plate morphology. However, the ettringite in M0 concrete has not been consumed. This could be attributed to dicalcium silicates that do not hydrate at initial hardening were trapped by sulfates to form ettringite after concrete has hardened, due to available moisture in M0 concrete. However, higher alumina and finer particles in IOT help greatly retards the reaction and formation of ettringite. This is an indication that IOT contributed to the densification of the microstructure of the respective concrete due to its micro-filling ability.

4 Conclusions

Due to the high affinity of IOT for water demand, there was significant decrease in the slump of the IOT concrete, which was believed, influenced by the surface area and rough surface of the tailings, but the addition of superplasticiser has improved the cohesiveness. The concrete sample M50 produced the highest value of compressive strength, 37.7 MPa, which gave higher strength than M0 concrete sample, which serves as reference. They all attained the designed strength of grade 30 at 28 days curing.The flexural strength of IOT concrete increased with increase in IOT up to the optimum and then decreased. However, all the values were higher than control specimen. The XRD results revealed the consumption of $Ca(OH)_2$ in IOT concrete during the hydration process and formation of more C-S-H gel in all replacement levels, leading to increase in strength. The morphology of the bulk concrete matrix clearly depicted the influence of the IOT. There was a consistent decrease in calcium hydroxide content with densification of the matrix as a result of increased volume of C-S-H. This has contributed to the achievement of higher compressive strength.

The authors are grateful to Ministry of Education (MOE) and Research Management Centre (RMC), Universiti Tecknologi Malaysia (UTM) for providing the Research University Grant (RUG), Vot. No: Q. J13000. 2509. 06H5

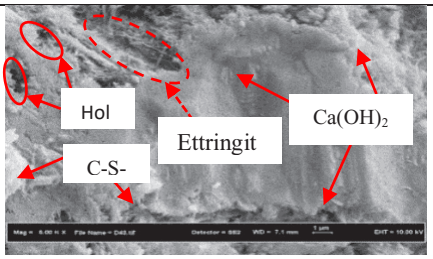

Fig. 7. Microstructure of M0 concrete

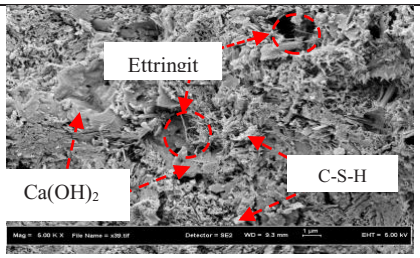

Fig. 8. Microstructure of M25 concrete

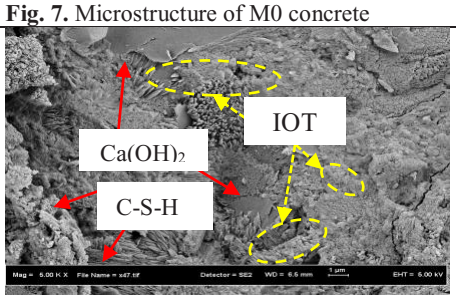

Fig. 9. Microstructure of M50 concrete

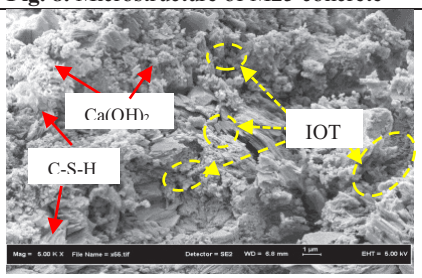

Fig. 10. Microstructure of M75 concrete

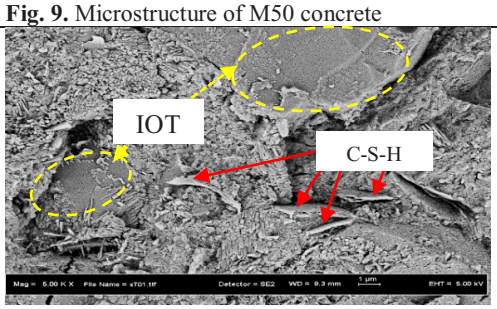

Fig. 11. Microstructure of M100 concrete at 28 days

References

1. Y.F., Hou, X. Jia, Adv Materials Res **671-674**, 1856-1859 (2013)
2. H.Z., Kang, K.W. Jia, L. Yao, Appl Mech Mater, **148-149**, 904-907 (2011)
3. A.T., Ako, S.U. Onoduku, A.S. Oke, I.B. Essien, N.F. Idris, N.A. Umar, A.A. Ahmed, J Geosci Geom, **2** (2), 42-49 (2014)
4. M., Edraki, , T. Baumgartl, E. Manlapig, D. Bradshaw, D.M. Franks and C.J. Moran, J Clean Prod **84**, 411-420 (2014)
5. L., Yu, J.S. Tian, J.X. Zhang and R.J. Yang, Adv Materials Res **250-253**, 1017-1024 (2011)
6. ASTM C494, *American Standard Testing of Materials - Standard Specification for Chemical Admixtures for Concrete*. American society of testing and materials Publication, 10 (2013)
7. BS EN 12350-2, *Testing fresh concrete (Slum test).* BSI Standards Publication, London (2009)
8. BS 1881-103, *Method for determination of compacting factor*. BSI Standards Publication, London (1993)
9. BS EN 12350-6, *Testing fresh concrete density*. BSI Standards Publication, London (2009)

10. ASTM C33, *American Standard Testing of Materials - Specification for Concrete Aggregates*. American society of testing and materials Publication, 11 (2003)
11. M., Yellishetty, V. Karpe, E.H. Reddy, K.N. Subhash, P.G. Ranjith, Resour Conserv Recy **52**(11), 1283-1289 (2008)
12. G.D., Zhang, X.Z. Zhang, Z.H. Zhou and X. Cheng, Adv Materials Res **838-841**, 152-155 (2013)
13. T.I., Ugama, S.P., Ejeh, International Journal of Advances in Engineering & Technology **7** (4), 1170-1178 (2014)
14. B.N.S., Kumar, R. Suhas, S.U. Shet and J.M. Srishaila, International Journal of Research in Engineering and Technology, **3** (7), 369-376 (2014)
15. M., Manjula, H.S. Sachin, K.M. Shivakumar, D.R. Ranjitha, B.M. Santhosh, International Journal of Informative & Futuristic Research, **2** (10), 3802-3812 (2015)
16. BS 5328-1, *Guide to specifying concrete*. BSI Standards Publication (1997)
17. Neville, A.M., *Properties of concrete*, Pearson Education Limited, London (2011)